



ELSEVIER

Available online at www.sciencedirect.comGLOBAL AND PLANETARY
CHANGE

Global and Planetary Change xx (2007) xxx–xxx

www.elsevier.com/locate/gloplacha

Strength and spatial patterns of the Holocene wintertime westerlies in the NE Atlantic region

Jostein Bakke^{a,b,*}, Øyvind Lie^a, Svein Olaf Dahl^{a,b},
Atle Nesje^{a,c}, Anne Elisabeth Bjune^d

^a Bjercknes Centre for Climate Research, Allégaten 55, N-5007 Bergen, Norway

^b Department of Geography, University of Bergen, Fosswinckelsgt. 6, N-5020 Bergen, Norway

^c Department of Earth Science, University of Bergen, Allégaten 41, N-5007 Bergen, Norway

^d Department of Biology, University of Bergen, Allégaten 41, N-5007 Bergen, Norway

Received in revised form 9 June 2006; accepted 14 July 2006

Abstract

Two records of July temperature and two records of reconstructed winter precipitation along the western coast of Norway have been combined to examine regional patterns in glacier activity and winter precipitation during the Holocene. The maritime glaciers in western Norway are mainly controlled by winter precipitation. Hence, fluctuations in magnitude and equilibrium-line altitude (ELA) of these glaciers reflect variability in wintertime atmospheric circulation patterns in the northeast Atlantic region. By combining an independent proxy for summer temperature with reconstructed ELAs during the Holocene, it is possible to reconstruct former winter precipitation. We track the dominant position of the westerlies during the Holocene by comparing records of winter precipitation along a 2000 km south–north coastal transect in Norway. Analyses of modern data on the evolution of the polar vortex indicate that there is a strong relationship between polar vortex and storm-track variability over the North Atlantic. Periods with increased winter precipitation along the coast of Norway are associated with a stronger effect of the westerlies, where differences in the distribution of precipitation are assumed to reflect changes in the position of the westerlies. The largest precipitation anomalies caused by a dominant southerly position of the westerlies are found around 2.8, 1.2 and 0.4 ka yrs BP. However, a general humid phase prevailed between 2.3 and 0.9 ka yrs BP.

© 2007 Elsevier B.V. All rights reserved.

Keywords: glacier variations; lake sediments; polar vortex; westerlies; Neoglacial; large-scale atmospheric circulation; eastern North Atlantic; climate; North Atlantic Oscillation

1. Introduction

The largest projected future climatic change because of anthropogenic forcing is expected to take place at

higher latitudes (Cubasch et al., 2001). Hence, the North Atlantic region is a key area for climate research, and the numbers of palaeoclimatic records reflecting climate variability from this region have increased significantly over the latest decade (e.g. Jansen et al., 2004). However, proxies for Holocene winter climate is sparse as most of the marine and terrestrial proxies respond to the summer season (e.g. Seppä and Birks, 2001, 2002; Andersson et al., 2003; Risebrobakken et al., 2003;

* Corresponding author. Bjercknes Centre for Climate Research, Allégaten 55, N-5007 Bergen, Norway. Tel.: +47 55 58 98 32; fax: +47 55 58 43 30.

E-mail address: Jostein.Bakke@geog.uib.no (J. Bakke).

Andersen et al., 2004; Bjune et al., 2004, 2005). One of few proxies for reconstruction of climate during the winter season backwards in time is changes in equilibrium-line altitudes (ELAs) at small glaciers. By combining an independent proxy for summer temperature with reconstructed ELAs during the Holocene, it is possible to reconstruct former winter precipitation (Dahl and Nesje, 1996). Over decadal timescales, changes in the North Atlantic Oscillation (NAO) index are strongly related to variations in storminess and winter precipitation in southern Norway (Hurrell, 1995; Hurrell et al., 2003). Glacier fluctuations in south-western Norway have therefore been suggested as a palaeo-indicator for low-frequent variations in the NAO (e.g. Nesje et al., 2000b). During the latest years, however, it is shown that one of the two polarities of the leading mode of the North Atlantic storm-track variability corresponds to a blocking situation of the NE Atlantic with a strong north-eastward tilt of the storm-track axis and reduced precipitation in western Europe. This situation is, however not captured by standard NAO indices (Rogers, 1997; Shabbar et al., 2001), and reanalyses using data of geopotential height, air temperature, wind and precipitation for the high-latitude Northern Hemisphere suggests that it is necessary to include the state of the polar vortex in any study of North Atlantic climate variability (Graf and Walter, 2005; Walter and Graf, 2005). Walter and Graf (2005) suggest that precipitation anomalies at the west coast of Greenland and the anomalies at the Norwegian coast could serve as a proxy for the strength of the polar vortex. Their reanalysis data shows enhanced precipitation in these regions during periods with a strong state of the polar vortex, and a significant reduced precipitation in south-western Norway during periods with a weaker state. Hence, when the polar vortex is strong, a basin-wide tripole correlation between tropospheric variability and sea-surface temperatures (SST) is seen in the North Atlantic. The importance of wind stress and atmospheric modes have also been emphasised for the Atlantic meridional overturning circulation (AMOC) during recent years (Dickson et al., 2000; Timmermann and Goosse, 2004). Hence, independent information on atmospheric behaviour has impact for natural systems also outside the terrestrial realm.

In this paper we present data on reconstructed glacier activity and winter precipitation along a coastal south–north transect in Norway. Several site-specific glacier reconstructions have been published from Scandinavia during the latest decades (Nesje et al., 2007–this issue and references therein). Here, we use data on glacier fluctuations and winter precipitation in order to discuss

regional patterns that can unlock the non-stationary behaviour of the North Atlantic winter atmospheric circulation (e.g. Barnston and Livezey, 1987; Luterbacher et al., 1999, 2002; Dawson et al., 2002; Ostermeier and Wallace, 2003; Cassou et al., 2004). Three different aspects will be discussed based on the data extracted from reconstructed glacier variations and winter precipitation from southern to northern Norway: 1) The overall conditions for glacier growth along the western coast of Norway in relation to possible forcing mechanisms during mid to late Holocene. 2) Large-scale Holocene changes in the strength of the westerlies based on a humidity index for Scandinavia, reflecting the total amount of winter precipitation received along the western coast of Norway. 3) Winter precipitation anomalies along the western coast of Norway in relation to large-scale changes in atmospheric circulation patterns with especial emphasis on the main track of the prevailing westerlies in the NE Atlantic region.

2. Study area, data validation and methods

Data on ELA fluctuations and winter precipitation used in this paper originate from the glaciers Northern Folgefonna (24 km²) on the Folgefonna Peninsula (60°N 06°E) in southern Norway and Lenangsbreene (c. 2 km²) on the Lyngen Peninsula (69°N 20°E) in northern Norway (Fig. 1). The glacier reconstructions are based on studies of distal-fed glacier lakes (Bakke et al., 2005a,b,c). Both Northern Folgefonna and Lenangsbreene are small temperate glaciers with a relative short frontal response time (ca 10 yrs.). Essential when using sediment records containing sediments from distal-fed glacier lakes is that the upstream glacier has no storage of sediments within the ice. This is established at both sites, as the glaciers are temperate and situated on non-calcareous Precambrian rocks in steep terrain. The two glacier records are based upon an identical multi-proxy sediment analysis based on loss-on ignition, bulk density, magnetic susceptibility and grain-size distribution. Dating is performed by AMS radiocarbon dates on both macrofossil and bulk samples (Table 1). The glacial component of the sediments is separated through multi-proxy analysis. The validated dry bulk density (DBD) records are then transformed into a continuous glacier reconstruction through a regression model elucidating the relationship between known ELAs (e.g. dated moraines; present glacier size, onset of the Neoglacial) and dry bulk density (DBD) (Bakke et al., 2005a,b,c).

Winter precipitation is calculated based on a close exponential relationship between mean ablation-season temperature (1 May–30 September) and mean solid

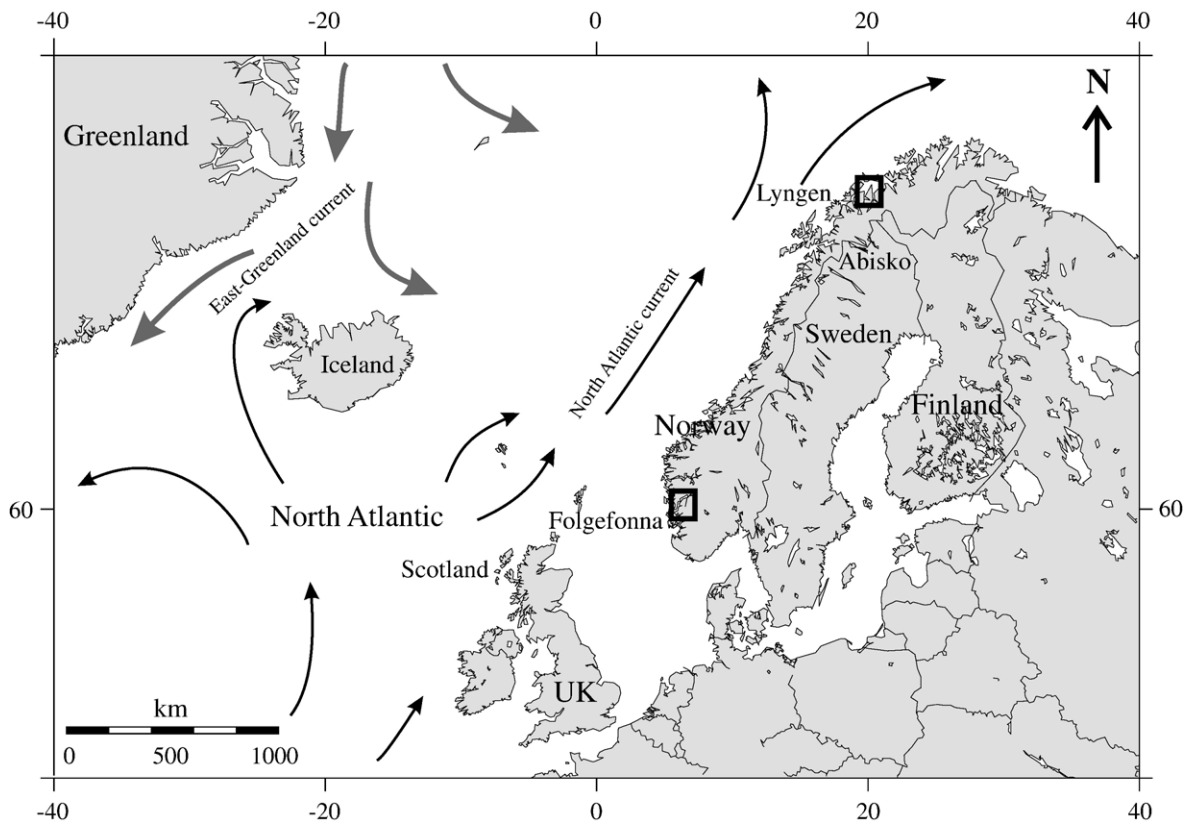


Fig. 1. The eastern North Atlantic region. The black squares mark the study areas on the Folgefonna Peninsula in southern Norway and the Lyngen Peninsula in northern Norway. The two sites are separated by 2000 km.

winter precipitation (1 October–30 April) at the ELA of Norwegian glaciers in maritime to continental climatic regimes (Liestøl in [Sissons, 1979](#); [Sutherland, 1984](#)). The relationship is expressed through the “Liestøl equation” that implies that if the former ELA is known, it is possible to quantify how the winter precipitation has fluctuated if an independent proxy for mean ablation-season temperature is used in the calculation ([Dahl and Nesje, 1996](#)). The validity of this relationship over a longer time span than the data used in the equation is tested by [Lie et al. \(2003b\)](#).

As an independent proxy for summer temperature we have used two pollen reconstructions based on transfer functions, one from the western Folgefonna Peninsula in southern Norway and one from Skibotn just east of the Lyngen Peninsula in northern Norway ([Bjune et al., 2004, 2005](#)). The pollen-climate surface data set includes data from 191 lakes distributed throughout Norway and northern Sweden (H.J.B. Birks, S.M. Peglar and A. Odland, unpublished data) and 113 lakes from Finland ([Seppä et al., 2004](#)). They are both calculated based on the same method using a weighted-

averaging partial least squares (WA-PLS) regression. The resulting two-component modes have a good predictive ability as estimated by leave-one-out cross-validation. July temperature has an estimated uncertainty of ca 1 °C within two standard errors in the transfer functions ([Birks, 2003](#)). As the pollen transfer function data express July temperature, we have used variations in δ July temperature compared with present mean ablation-season temperature in our calculation. This may overestimate some of the variance since July temperature may have higher variance than mean ablation-season temperature. However, regression between mean ablation summer temperature and July temperature shows a close relationship both in southern and northern Norway with $r=0.74$ and $r=0.67$, respectively (during the last normal period; 1961–1990).

A common problem when obtaining continuous records of former winter precipitation from glacier archives is that all glaciers studied in Scandinavia were melted away for shorter or longer time span(s) during the Holocene ([Nesje et al., 2007-this issue](#)). During periods with no glacier, the reconstructed winter

Table 1

Radiocarbon dates used in this study (also published in Bjune et al., 2005; Bakke et al., 2005a,b,c). For the two pollen records age–depth relationships were established by the use of a mixed model approach (Heegaard et al., 2005), whereas the age–depth relationships for the glacial records were established by linear interpolations

	Lab number	Depth (cm)	Type of material	¹⁴ C age	2.σ cal yr BP
Vestre Øykjamyra	Poz-801	34–35	Plant macrofossils	235±45	141–444
	Poz-805	82–83	Plant macrofossils	1530±30	1350–1470
	Poz-803	130–131	Plant macrofossils	2830±40	2890–2985
	Poz-802	178–179	Plant macrofossils	4590±45	5240–5380
	Poz-804	201–202	Plant macrofossils	5930±50	6660–6830
	Poz-799	217–218	Plant macrofossils	6880±50	7620–7740
	Poz-800	227–228	Plant macrofossils	7630±55	8385–8430
	Poz-806	241–242	Plant macrofossils	7990±55	8740–9025
	Poz-813	302–303	Plant macrofossils	10 070±50	11 325–11 885
	Poz-811	332–333	Plant macrofossils	10 730±60	12 720–13 010
	Poz-1162	354–356	Plant macrofossils	11 170±60	13 070–13 230
Vetlavatn core I	Tua-13603A	15	Bulk sediments	6785±160	7470–7935
	Tua-13604A	20	Bulk sediments	7475±30	7790–8785
	Tua-13605	33	Bulk sediments	7640±135	8315–8500
	Tua-13606	46	Bulk sediments	8950±145	9860–10 035
	Beta-115399	50	Bulk sediments	8840±60	9850–9920
	Beta-115400	53	Bulk sediments	8990±60	9940–10 005
	Beta-115401	58	Bulk sediments	9050±60	9975–10 035
	Beta-115403	61.5	Bulk sediments	9660±70	10 625–10 960
Vetlavatn III	Beta-115403	69.5	Bulk sediments	10 200±80	11 680–12 155
	Beta-148430	110	Bulk sediments	9630±60	10 690–11 160
Vetlavatn IV	Beta-148431	118	Bulk sediments	10 250±70	11 580–12 360
	Beta-148424	23	Bulk sediments	2980±40	3000–3260
Vetlavatn IV	Beta-148425	118	Bulk sediments	8150±50	8990–9130
	Beta-148426	136	Bulk sediments	9360±60	10 270–10 670
	Beta-148427	138	Bulk sediments	9380±60	10 380–10 690
	Beta-148428	144	Bulk sediments	9830±60	11 130–11 250
	Beta-148429	148	Bulk sediments	10 480±40	12 080–12 820
	Vassdalsvatn 1	Beta-102930	28–31	Bulk sediments	1150±70
Beta-102931		117–120	Bulk sediments	2280±60	2160–2350
Beta-102932		182–185	Bulk sediments	3370±70	3480–3690
Beta-102933		250–253	Bulk sediments	4270±80	4650–4965
Beta-102934		295–298	Bulk sediments	5200±70	6170–6590
Beta-102935		368–372	Bulk sediments	8260±80	9130–9415
Beta-102936		525–535	Bulk sediments	4330±50	4840–4965
Vassdalsvatn 2	Tua-13607	19	Bulk sediments	2100±85	1970–2295
	Tua-13608	83–84	Bulk sediments	1900±70	1735–1920
	Tua-13788A	77–79	Bulk sediments	2310±60	2160–2360
	UtC-6691	123	Bulk sediments	2765±45	2785–2920
	UtC-6692	138	Bulk sediments	3319±40	3475–3630
	UtC-6693	142	Bulk sediments	3460±60	3640–3830
	UtC-6694	147	Bulk sediments	3820±50	4100–4345
	UtC-6695	171	Bulk sediments	6280±60	7030–7270
Dravladalsvatn I	Poz-3175	1	Plant macrofossils	2060±30	1990–2060
	Tua-3627A	24	Bulk sediments	2000±40	1920–1990
	Tua-3628A	57	Plant macrofossils	2315±45	2305–2355
	Poz-3176	72	Plant macrofossils	5530±40	6290–6390
	Poz-3177	82	Bulk sediments	8090±40	9000–9220
	Tua-3629A	88	Bulk sediments	8645±70	9540–690
	Dravladalsvatn II	Poz-3178	1	Bulk sediments	2565±30
Tua-3640A		24	Bulk sediments	2320±45	2180–2360
Poz-3198		45	Bulk sediments	2315±25	2330–2350
Tua-3630		78	Plant macrofossils	1910±45	1745–1910
Tua-3631A		100	Bulk sediments	3215±60	3360–3475
Poz-3179		124	Bulk sediments	4675±35	5320–5465
Poz-3256		132	Bulk sediments	5050±30	5805–5890

Table 1 (continued)

	Lab number	Depth (cm)	Type of material	¹⁴ C age	2.σ cal yr BP
Aspvatn I	Tua-3632A	151	Bulk sediments	6375±70	7250–7415
	Beta-154058	66–65	Bulk sediments	5830±40	6630–6670
	T-8987	66	Macrofossil	4220±45	4585–4860
	Beta-154059	100–99	Bulk sediments	7420±50	8160–8350
	Beta-154060	136–135	Bulk sediments	9210±40	10240–10500
	Beta-154061	182–180	Bulk sediments	10 160±40	11580–12290
	Beta-154827	182–180	Macrofossil (wood)	8010±40	8740–9020
	Beta-154062	211–210	Bulk sediments	11 070±50	12890–13180
	Beta-154063	245	Macrofossil	10 050±40	11300–11940
	Beta-154064	295	Shell	9220±80	10220–10575
Dalmutladdo	Beta-154065	480–478	Shell	9710±90	10740–11255
	Hela-499	6–7	Betula seeds	605±70	520–670
	Hela-508	22–23	Piece of wood	775±65	640–800
	Hela-500	48–49	Pinus needle	1725±65	1515–1820
	Hela-509	75–76	Scale, wood	2555±105	2350–2810
	Hela-513	113–114	Indet.	3495±65	3610–3920
	Hela-510	137–138	Pinus needle	4615±75	5050–5480
	Hela-502	173–174	Pinus needle	5620±85	6280–6570
	Hela-511	210–211	Betula leaves	7225±115	7840–8320
	Hela-503	226–227	Betula seeds, bark	7730±90	8370–8730
	Hela-512	247–248	Bark, Betula seeds	8110±120	8645–9325
	Hela-504	265–266	Betula leaves	8765±110	9550–10160

precipitation must consequently be expressed as maximum potential winter precipitation before a glacier reforms at the site. The altitude of instantaneous glacierization (AIG) (Lie et al., 2003a) adjusted for land uplift is used to calculate the maximum potential winter precipitation during these time spans. This is done by calculating the necessary winter precipitation for a glacier to reform based on the estimated summer temperature at the height of the highest mountain surrounding the glaciers (Lie et al., 2003a).

Time resolution on the four different records used in this study varies from 7 to 300 yrs throughout the Holocene, with lowest time resolution in the oldest part of the records. The data set for the last 5500 yrs is therefore harmonised to an average resolution of 50 yrs. During periods with lower time resolution than 50 yrs we have extrapolated between the data points, using a forecast model based on the linear trend. In periods with higher time resolution than 50 yrs we have smoothed the data using a lowness smoother function. The data set for mid and early Holocene is averaged in the same way to 100 yrs time resolution.

The chronological error varies from 50 to 150 yrs based on the different age–depth models (Bjune et al., 2004, 2005; Bakke et al., 2005a,b,c). However, since the winter precipitation data are derived from several independent sources, where all data are assembled, there is an accumulated age uncertainty of about 200 yrs.

In this study we only used continuous data from the Neoglacial period (defined as the onset of the glaciers after the thermal maximum in Scandinavia) as the records from the early Holocene lack continuous information (see above). During the early Holocene the sediment fluxes were significantly different from the late Holocene partly due to paraglacial reworking of old glacial sediments (Ballantyne, 2002), and partly due to large and abrupt glacier events (Bakke et al., 2005a). Sediment records retrieved from distal glacier-fed lakes during the first two millennia after Younger Dryas are therefore commonly difficult to resolve (Dahl et al., 2003).

It is important to be aware of the different sources of error when quantifying winter precipitation based on summer temperature and variations in glacier ELAs, as the method includes at least two different data sets, accumulating error estimates from both records. The main factors summarised are; 1) uncertainties in the temperature reconstructions, 2) uncertainties when reconstructing former ELA and 3) uncertainties in the relationship between ELA and sediment parameters. Therefore, a statistical standard error is difficult to achieve. Using four different radiocarbon-dated chronologies in the way used in this paper clearly introduces the problem of age uncertainties, as there is a relatively large age–depth error estimate on the proposed variance. The proposed variance between north and south should therefore be regarded as relative estimates.

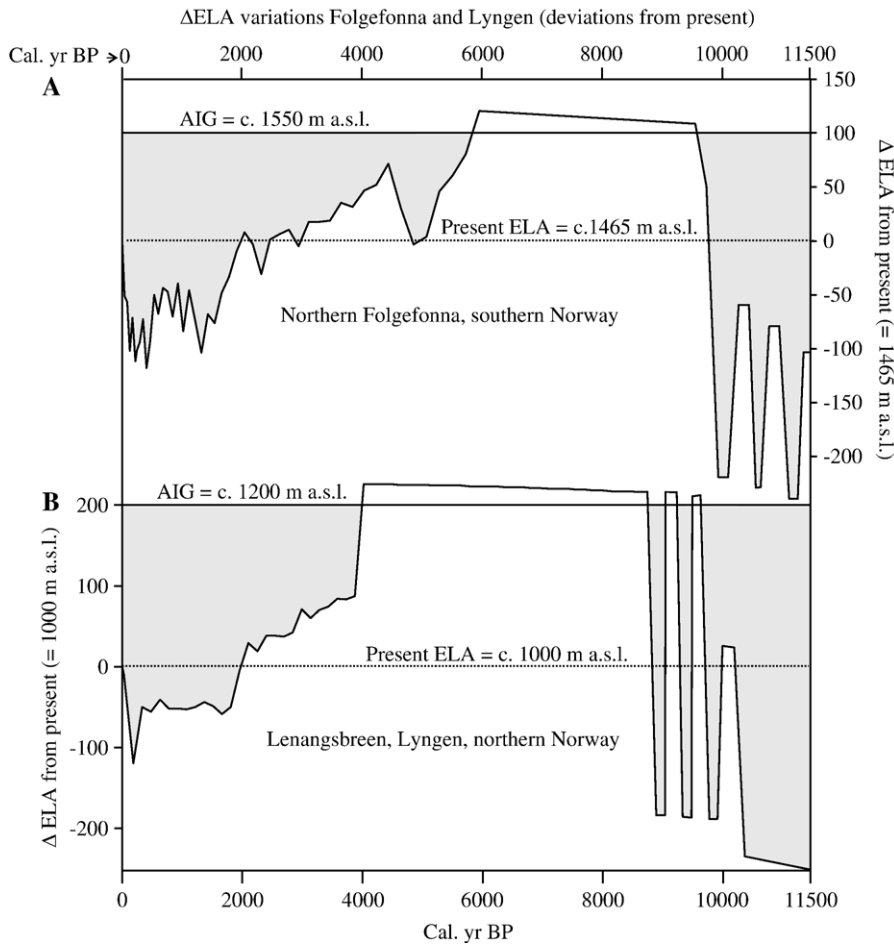


Fig. 2. A and B: reconstructed equilibrium-line altitudes (ELAs) from (A) Northern Folgefonna and (B) Lenangsbreen in Lyngen. Both records are based on lacustrine sediments from proglacial lakes. Upper panel in both figures; AIG=altitude of instantaneous glacierization.

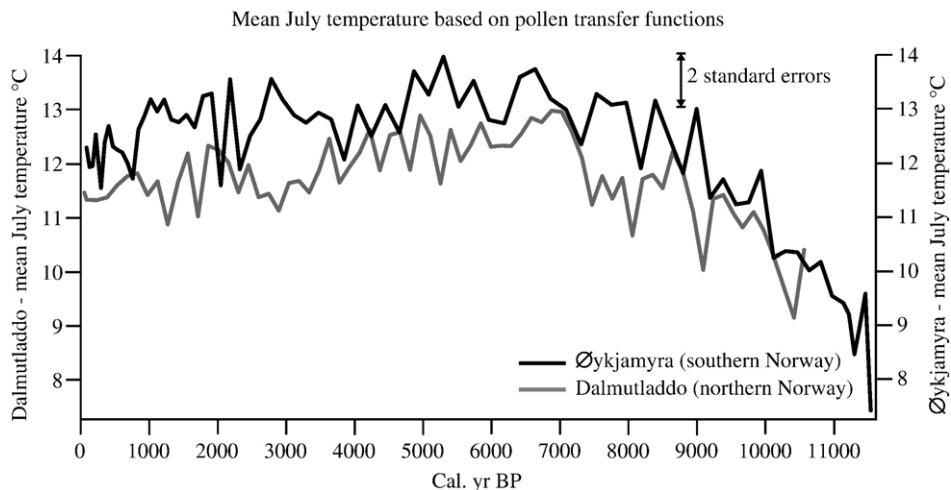


Fig. 3. Two pollen-based reconstructions of mean July temperature throughout the Holocene. During some periods there is a marked anti-phasing in the temperature development between southern and northern Norway.

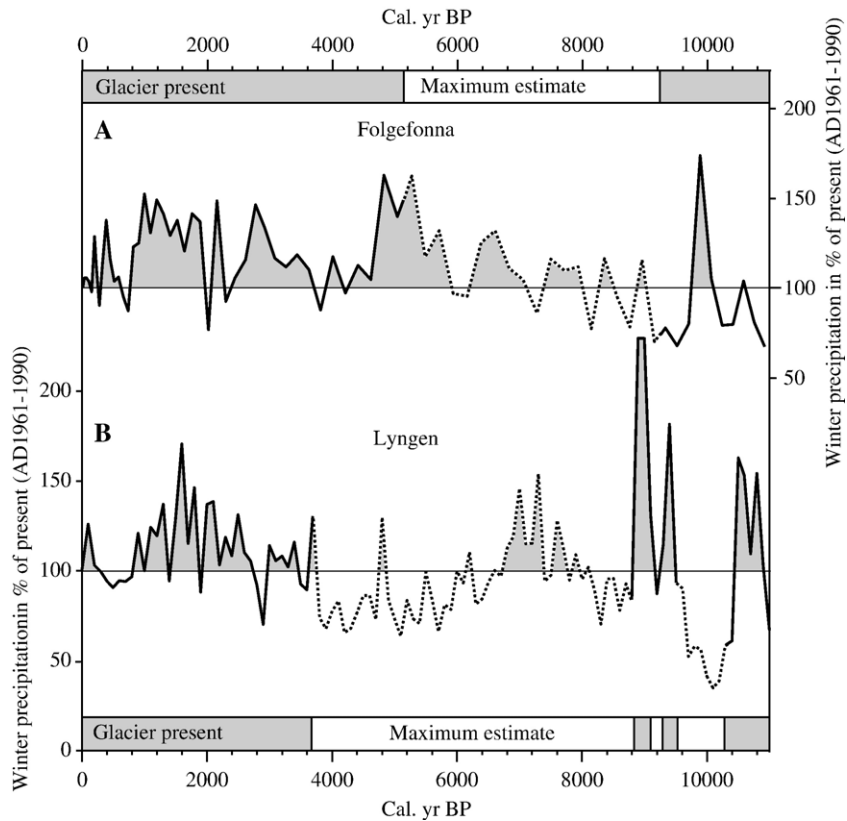


Fig. 4. A and B: reconstructed winter precipitation from (A) Folgefonna. Solid line corresponds to periods when the glacier is present whereas dotted line shows maximum potential winter precipitation during periods when the glacier was melted away. B: same as in figure A but from Lyngen.

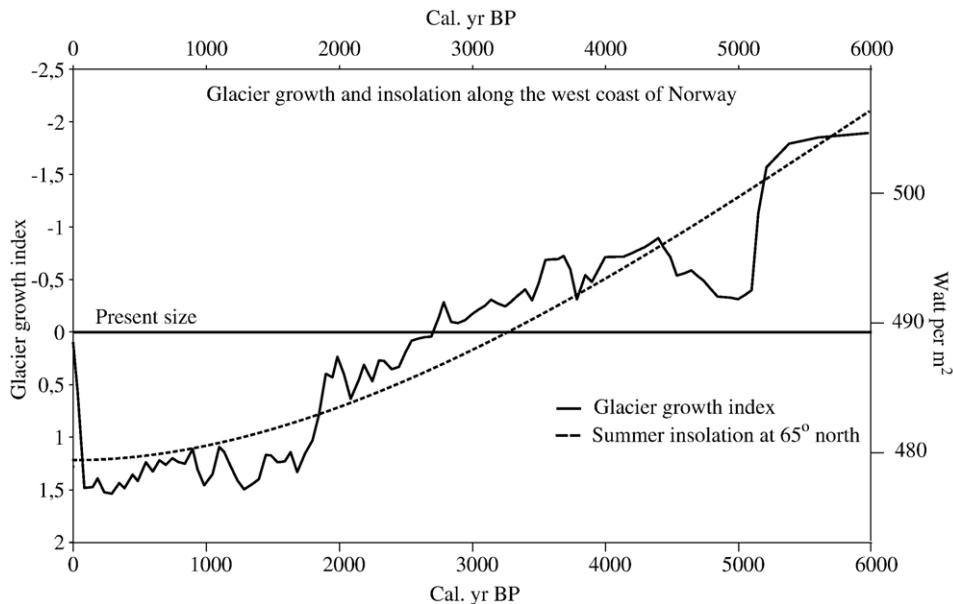


Fig. 5. Combined equilibrium-line altitude (ELA) variations along the south–north coastal transect in Norway. The glacier growth index is simply expressed by adding standardised ELA estimates from southern and northern Norway. The overall trend follows the insolation curve at 65°N, indicating that the overall conditions for glacierization are closely related to external forcing.

3. Results

3.1. Glacier variations along the coastal transect

3.1.1. Early Holocene (11 500–8000 cal. yr BP)

During the early Holocene a glacier event chronology based on radiocarbon dates within moraines, from bog deposits and from lake sediments from both southern and northern Norway has been established (Nesje et al., 1991; Dahl and Nesje, 1996; Nesje et al., 2000a, 2001; Dahl et al., 2002; Bakke et al., 2005a,b) (Fig. 2A). The glacial events in southern Norway occurred at 11 500 cal. yr BP, 10 500 cal. yr BP, 10 100 cal. yr BP, 9700 cal. yr BP and 8400–7900 cal. yr BP. In northern Norway the early Holocene glacial events took place at 10 400–10 300 cal. yr BP, 9800–9400 cal. yr BP and 9300–8900 cal. yr BP (Bakke et al., 2005b) (Fig. 2B). For the early Holocene it is possible to make good estimates of the winter precipitation during the glacial events. It is however, difficult to resolve winter precipitation in periods when the glaciers were

retreating, since ELAs were calculated with minimum estimates for initiating a glacier retreat, which could be an underestimate of the actual rise in ELA.

The pollen records from this time span indicate a gradual rise in temperature from around 4 °C cooler during the earliest Holocene to about present values around 8000 cal. yr BP (Bjune et al., 2004, 2005). Around 9000 cal. yr BP a marked anti-phase between south and north is detected between the two temperature records ca 9000 cal. yr BP and ca 8500 cal. yr BP (Fig. 3).

Reconstructed winter precipitation shows in general dry conditions, but with large precipitation anomalies up to 200% of present winter precipitation in northern Norway (Fig. 4). The most striking anti-phasing is seen close to 10 000 cal. yr BP when it was very dry in northern Norway simultaneously with a marked increase in winter precipitation in southern Norway. The strong winter season precipitation anomalies between southern and northern Norway can be explained by large-scale reorganisations of the atmosphere. It seems like the position of the westerlies had a persistent track towards

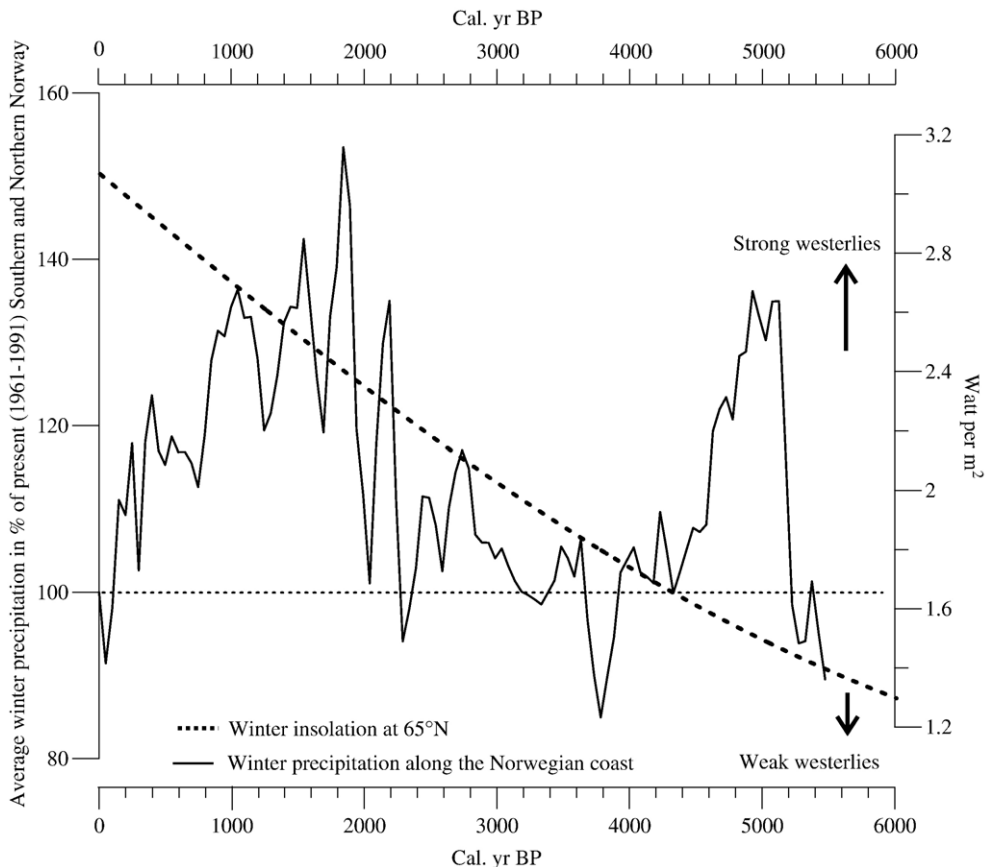


Fig. 6. The total amount of winter precipitation received along the coast of Norway constructed by dividing the winter precipitation estimates from Folgefonna and Lyngen by two. Dotted line shows average present winter precipitation in Lyngen and at Folgefonna.

southern Norway, whereas northern Norway was situated within the polar domain giving dry conditions.

3.1.2. Mid Holocene (8000–5200 cal. yr BP)

For shorter and longer time spans during the thermal maximum all studied glaciers in Scandinavia were melted away, probably as a combination of higher summer temperature and lower winter precipitation (Nesje et al., 2005, 2007–this issue). The records of winter precipitation during this time span are only valid as maximum potential precipitation estimates according to the height of the AIG. The precipitation could therefore have been much lower than what is indicated when the lines are broken (dotted) in Fig. 4. In Lyngen, Lenangsbreen melted ca 8900 cal. yr BP and the onset of the Neoglacial is radiocarbon dated to ca 3800 cal. yr BP. In southern Norway, Northern Folgefonna melted ca 9700 cal. yr BP. It is however, known from southern Norway that glaciers at higher altitude existed continuously to after the Finse Event (8.2 ka event) (Dahl and Nesje, 1996). The onset of the Neoglacial at Folgefonna started ca 5200 cal. yr BP. At Jostedalbreen (mainland Europe's largest ice cap) the onset of the Neoglacial is radiocarbon dated to ca 6000 cal. yr BP (Nesje et al., 2001).

The temperature records from 8000 to 5200 cal. yr BP show fluctuations around present values peaking in periods with 2 °C warmer than at present both in southern and northern Norway. From 8000 to 7200 cal. yr BP and ca 5200 cal. yr BP there was a marked anti-phasing in the reconstructed summer temperature from south to north. We suggest that this may be the response to a southward shift of the westerlies as arctic Scandinavia was dominated by polar air responsible for the cooling at higher latitude.

3.1.3. Neoglacial (~ 5200 cal. yr BP until present)

The first period of the Neoglacial was dominated by slowly growing glaciers. This period lasted from 5200 to 1800 cal. yr BP in maritime southern Norway, whereas in northern Norway it lasted from 3800 to 2000 cal. yr BP. During the latest 1800 cal. yr BP the ELA at Northern Folgefonna showed high-frequent fluctuations, with glacier magnitudes in periods larger than at present throughout the time span. There was a significant glacier maximum during the “Little Ice Age” (LIA) (AD 1400–1940). In Lyngen the ELA estimates were much more stable, with large glaciers and a marked maximum during the LIA starting ~AD 1750 ending close to AD 1900.

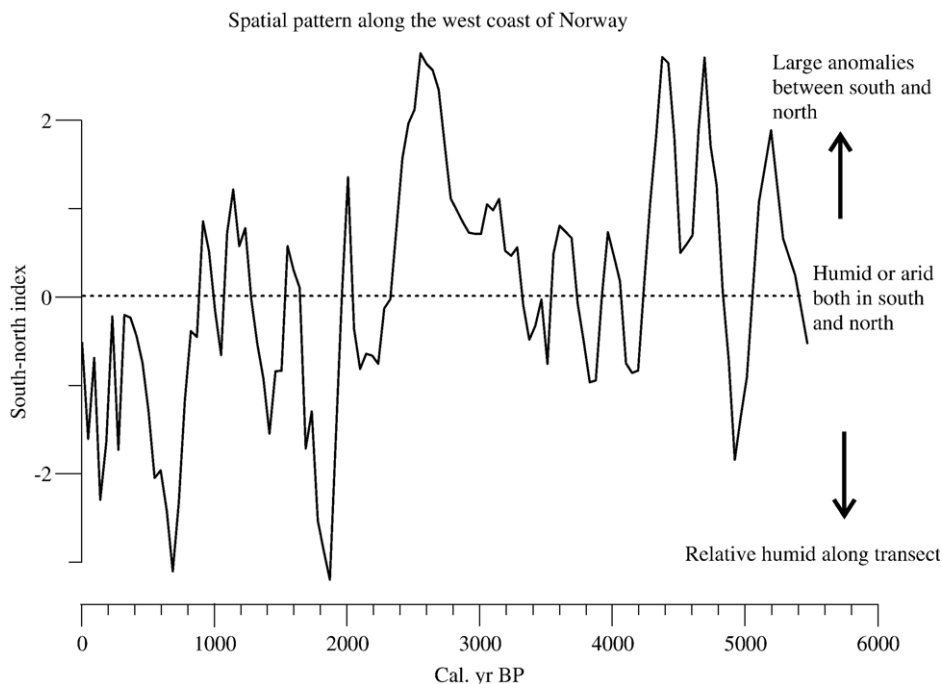


Fig. 7. The spatial pattern of winter precipitation along the south–north coastal transect. High values in index indicate dry conditions in northern Norway, whereas values close to zero indicate a low gradient (wet or dry both places). Low values indicate wet conditions along the entire western coast of Norway.

3.2. Conditions for glacier activity and winter precipitation anomalies along the S–N coastal transect

For the last 5500 cal. yrs BP we have examined reconstructed continuous time series of changes in ELA and winter precipitation in three different ways; (1) by showing the mean standardised ELA variations at Folgefonna and Lyngen ($FS_{\text{ela}} + LS_{\text{ela}}$) over the latest 5500 yrs BP in order to examine the mean glacier evolution along the maritime west coast of Norway (Fig. 5), (2) by evaluating the mean reconstructed winter precipitation-anomalies (percent from present normal period (1961–1990)) at Folgefonna and Lyngen ($FP_w + LP_w/2$) in order to explore the overall changes in precipitation along the west coast of Norway (Fig. 6), and (3) by subtracting the Folgefonna standardised winter precipitation from the Lyngen standardised winter precipitation ($FSP_w - LSP_w$) (Fig. 7) in order to examine relative geographical differences in winter precipitation distribution along the south–north transect that may provide information on large-scale atmospheric patterns.

4. Discussion

4.1. Equilibrium-line altitudes during the Neoglacial period

The overall evolution of maritime glaciers along the western coast of Norway is expressed in Fig. 5, showing a gradual decrease in ELA from 5200 cal. yr BP until the termination of the “Little Ice Age”. This pattern fits well with the general insolation curve for 65°N that may indicate a close linkage between glacier growth and solar orbital forcing at high latitudes during the late Holocene, also previously recorded in palaeoclimatic reconstructions from Scandinavia (e.g. Karlén and Kuylenssterna, 1996; Seppä and Birks, 2001; Korhola et al., 2002; Seppä and Birks, 2002; Andersen et al., 2004; Bjune et al., 2004). This pattern also turns up in model experiments simulating the Holocene climate evolution at high latitudes (Renssen et al., 2005). In marine records from the North Atlantic it is evident that the Holocene SST-evolution is increasingly associated to the summer orbital insolation-effect towards high-latitude areas (Kim et al., 2004). The change from a dry and warm mid Holocene into a wetter late Holocene occurred simultaneously with the increased dominance of Atlantic water along the western coast of Norway as seen from marine records (e.g. Risebrobakken et al., 2003). Wetter conditions combined with lower summer insolation made the climate favourable for glacier growth in

Scandinavia, especially at maritime sites along the North Atlantic coast of Norway (e.g. Nesje et al., 2001). However, superimposed on the forcing signature, high-frequent decadal to millennial scale climate fluctuations are observed in proxies from both the terrestrial (e.g. Nesje et al., 2005) and marine environment (e.g. Jansen et al., 2004; Nesje et al., 2005). Two sharp increases in glacier growth are seen close to 5000 and 1800 cal. yr BP. These two peaks can possibly be explained by higher winter precipitation as shown in Fig. 6. We conclude that the onset and general development of the Neoglacial at the western coast of Norway is a function of lower summer insolation and a gradually weakening of the seasonal amplitude as aphelion changes throughout the Holocene. We also emphasise that the retreat of maritime glaciers along the entire western Scandinavia over the last century is unprecedented in the entire Neoglacial period spanning the last 5200 years. Hence, this observation puts the reported glacier retreat in the 20th century (Oerlemans, 2005) into a long-time western North Atlantic perspective as an anomaly. However, some of the most maritime glaciers in Southern Norway with short response time to climate have shown expansion during the latest decade of the last millennium with a retreat towards the present. This is demonstrated to be a response to larger winter precipitation during some years in the early 1990s (Nesje, 2005).

4.2. Humidity index along the coastal transect

The average winter precipitation along the western coast of Norway is used as a relative humidity index (Fig. 6) expressing the mean changes in received precipitation. There was a significant peak in humidity close to 1800 cal. yr BP before it descends towards present values. Because the regional precipitation and winter accumulation at glaciers in western Norway is intimately associated to the westerly wind-field (Nordli et al., 2005), we explain this as an overall increase in the strength of the westerlies. Large glaciers are reported from maritime sites in both southern and northern Norway during the time span with maximum precipitation (Dahl and Nesje, 1996; Nesje et al., 2000a, 2001; Bakke et al., 2005b,c). SST data from the North Atlantic indicate increased variability during the same time span (Calvo et al., 2002), indicating higher variability in the atmospheric circulation, which possibly can be explained with higher intensification of the westerlies. A study of lake-level variations in west-central Europe also indicate higher lake levels in the same periods as we propose stronger westerlies over the North Atlantic region (Holzhauser et al., 2005).

4.3. Winter precipitation anomalies along the western coast of Norway — relation to polar vortex regimes

Variations in winter precipitation between two sites can be used to derive information on the overall changes in atmospheric circulation through time. As the maritime glaciers at the west coast of Norway are dependent on the supply of solid winter precipitation, their development is closely related to the wind fields and directions (Nordli et al., 2005). Based on this we have calculated a south–north coastal index for elucidating possible changes in atmospheric circulation through time.

The south–north coastal index expresses the regional distribution of precipitation along the western coast of Norway. It is evident that there is a persistent quasi-periodic behaviour in the distribution (Fig. 7). Close to 2000 cal. yr BP there was a shift from high to low gradient in winter precipitation along the 2000 km transect. It has been shown that the North Atlantic Oscillation (NAO) to a large extent controls the storminess at mid-latitudes in the North Atlantic region with increased storminess (and precipitation) during positive NAO scenarios and decreased storminess (and precipitation) during negative NAO periods (Hurrell, 1995; Dawson et al., 2002; Hurrell et al., 2003). Several studies have, however, demonstrated that this simple

relationship is influenced by the non-stationary behaviour of the atmosphere (e.g. Dawson et al., 2002; Cassou et al., 2004). This non-stationary behaviour over the 20th century has been associated to variations in sea-ice (Dawson et al., 2002). Moreover, the occurrence of multiple atmospheric patterns in the North Atlantic region has regained much attention over the last few years (e.g. Jacobeit et al., 2003). Similarly, Hutterli et al. (2005), showed that different regions of the Greenland Ice Sheet respond to different atmospheric anomaly-patterns in the North Atlantic. Recently, Casty et al. (2005) have also demonstrated that the NAO is only temporally robust over the last 500 years, and that other atmospheric circulation modes may dominate periodically over central Europe. See also Luterbacher et al. (1999, 2002) and Jacobeit et al. (2003) that there are other circulation patterns of relevance.

The strength of the polar vortex has been discussed as a forcing mechanism on the climate variability over the North Atlantic region and also as a mechanism to explain large-scale teleconnection patterns (Graf and Walter, 2005; Walter and Graf, 2005). The polar vortex is a persistent large-scale cyclonic circulation pattern in the middle and upper troposphere and the stratosphere, centred generally in the polar regions of each hemisphere. In the Arctic, the vortex is asymmetric and

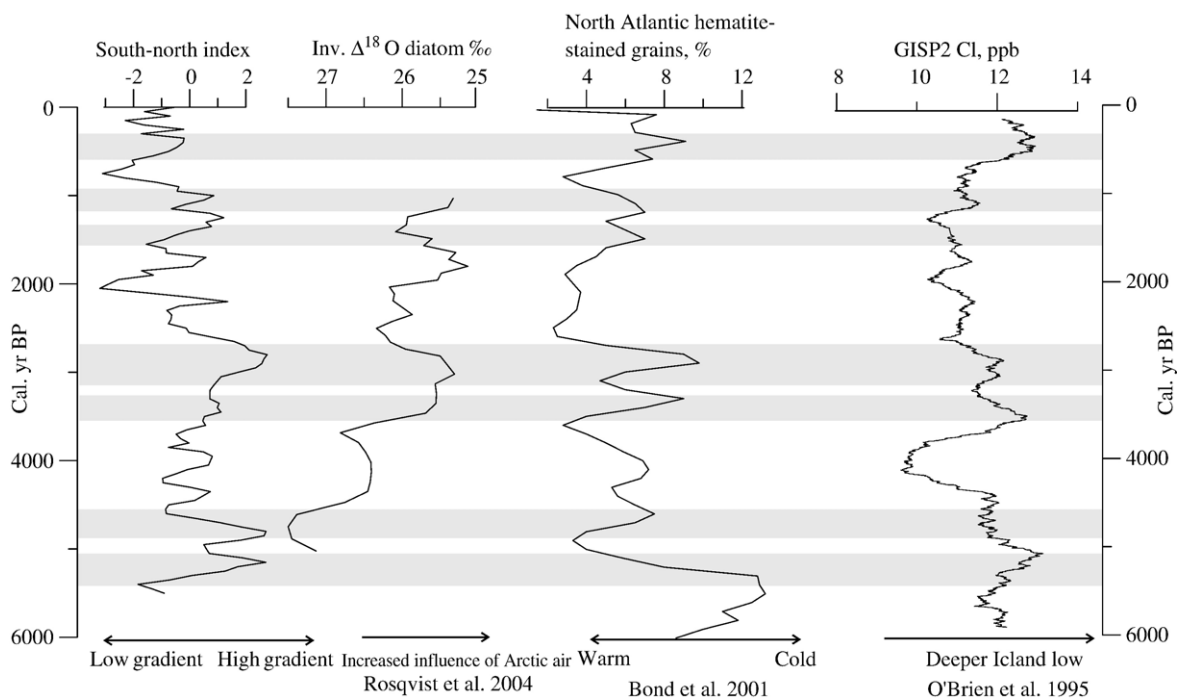


Fig. 8. Comparison between the south–north coastal index, oxygen isotope values on diatoms from northern Sweden (Rosqvist et al., 2004), Ice Rafted Debris (IRD) from the North Atlantic (Bond et al., 2001) and Cl from the GISP2 ice core (O'Brien et al., 1995). Apparently, all records are influenced by the general atmospheric circulation in the North Atlantic region, and are therefore expected to share some common trends.

typically features a trough over the Northern Hemisphere. However, it is important to have in mind that the polar vortex is not a surface pattern, but tends to be well expressed at upper levels of the atmosphere and wheels the arctic polar jet streams. During periods with strong polar vortex regimes, higher pressure at mid-latitudes drives ocean storms farther north, and changes in the circulation pattern bring humid winter weather to Alaska, Scotland and Scandinavia, as well as drier conditions to the western United States and the Mediterranean (Walter and Graf, 2005). We therefore propose the strength of the polar vortex as a possible mechanism to explain the large-scale winter precipitation anomalies between southern and northern Norway. A chemical record from the GISP2 ice core from Greenland is inferred to express the deepening of the Icelandic Low (Mayewski et al., 2004) (Fig. 8). Another archive from the North Atlantic suggested to be influenced by the general circulation pattern over the North Atlantic region, is the amount of ice rafted debris (IRD) in marine cores to the west of Scotland (Bond et al., 2001). Periods with large amounts of IRD correspond (see the gray shaded sub-periods in Fig. 6) to periods when our data suggests that there was a high winter precipitation gradient between southern and northern Norway and to periods when the GISP2-record indicate increased deepening of the “Icelandic low”. This demonstrates that sea-ice may partly respond to or force the atmospheric anomaly-patterns we observe. Data on diatom oxygen isotope variations from sediments in a proglacial lake in northern Sweden is inferred to reflect influence of Arctic air in northern Scandinavia (Rosqvist et al., 2004). The variations in these data are in sub-periods comparable with our south–north index, peaking into lower isotope values during the same time span as periods with a high gradient between southern and northern Norway. Especially the period centred around 3000 cal. yr BP corresponds with the south–north index.

We note that the spatial gradient between southern and northern maritime Norway is associated to a suite of well-known records that have been attributed to atmospheric polar regimes. However, whereas the rate of advection is taken out from our south–north gradient, the site-specific records we have compared with contain also variations in strength. Moreover, whereas our record is strictly seasonal, the site-specific records are more ambiguous in terms of which season they respond to. This indicates that the millennial-scale signature in these records are to a large degree explained by non-stationary shifts in atmospheric circulation patterns that in turn give spatial anomaly-patterns on precipitation and air-masses over the North Atlantic region. Our results therefore

emphasise the need to constrain the seasonal response of different proxy archives, the spatial patterns that are involved in Holocene climate variations as well as variations in the strength of the atmospheric circulation.

5. Conclusions

Based on the data analyses and the above discussion, the following conclusions of local and regional importance are suggested:

1. The retreat of maritime glaciers along western Scandinavia over the last century is unprecedented in the entire Neoglacial period spanning the last 5200 yrs.
2. Four AMS radiocarbon-dated chronologies are used to reconstruct and analyse glacial condition, humidity, and winter precipitation gradients along a south–north coastal transect in Norway in order to shed light on the general atmospheric circulation patterns over the North Atlantic region during the Holocene.
3. Early Holocene shows large-scale shifts in winter precipitation from southern to northern Norway based on the glacier event chronology derived through moraine chronologies, raised bogs and the study of lake sediments.
4. During the Holocene thermal maximum no reliable winter precipitation estimates can be retrieved as it is only possible to reconstruct the maximum amount of winter precipitation before initiating glacier formation.
5. The general conditions for glaciations along the western coast of Norway is responding to a slowly relaxation in orbital forcing. As the perihelion moved towards the winter, it became ideal conditions for glacier growth at maritime glaciers with mild and humid winters and relatively cold summers.
6. The total amount of winter precipitation along the western coast of Norway shows a marked peak in winter precipitation close to 5000 and 1800 cal. yr BP with a decrease towards present values. This is interpreted as a response to increased strength of the westerlies in the North Atlantic region.
7. The south–north index expresses geographical changes in winter precipitation distribution along the western coast of Norway. The entire record spanning the last 5500 cal. yr BP shows a quasi-periodic behaviour with large fluctuations from one century to the next. Around 2000 cal. yr BP there was a marked shift to wetter conditions and lower precipitation-gradients between southern and northern Norway.
8. There is some notable coherency in sub-periods between the south–north index, IRD in the North Atlantic, Cl from the GISP2 ice core, and oxygen

isotope measurements from a proglacial lake in northern Sweden, indicating a common response to large-scale atmospheric patterns.

9. Geographically distributed proxy records have the potential to resolve large-scale atmospheric patterns during the Holocene by reconstructing the spatial distribution and gradients between sites.

Acknowledgements

This is a contribution from NORPEC—a NFR funded strategic university project at the University of Bergen, co-ordinated by Professor John Birks, and to the NFR funded NORPAST-2 project coordinated by Professor Morten Hald. This is publication no. A 139 from the Bjerknes Centre for Climate Research.

References

- Andersen, C., Koç, N., Jennings, A., Andrews, J.T., 2004. Nonuniform response of the major surface currents in the Nordic Seas to insolation forcing: implications for the Holocene climate variability. *Paleoceanography* 19. doi:10.1029/2002PA000873.
- Andersson, C., Risebrobakken, B., Jansen, E., Dahl, S.O., 2003. Late Holocene surface ocean conditions of the Norwegian Sea (Voring Plateau). *Paleoceanography* 18 (2). doi:10.1029/2001PA000654.
- Bakke, J., Dahl, S.O., Nesje, A., 2005a. Late glacial and early-Holocene palaeoclimatic implications based on reconstructed glacier fluctuations and equilibrium-line altitudes at northern Folgefonna, Hardanger, western Norway. *Journal of Quaternary Science* 20 (2), 179–198.
- Bakke, J., Dahl, S.O., Paasche, Ø., Løvlie, R., Nesje, A., 2005b. Glacier fluctuations, equilibrium-line altitudes and palaeoclimate in Lyngen, northern Norway, during the Late glacial and Holocene. *The Holocene* 15 (4), 387–409.
- Bakke, J., Lie, Ø., Nesje, A., Dahl, S.O., Paasche, Ø., 2005c. Utilizing physical sediment variability in glacier-fed lakes for continuous glacier reconstructions during the Holocene, northern Folgefonna, western Norway. *The Holocene* 15 (2), 161–176.
- Ballantyne, C.K., 2002. Paraglacial geomorphology. *Quaternary Science Reviews* 21 (18–19), 1935–2017.
- Barnston, A.G., Livezey, R.E., 1987. Classification, seasonality and persistence of low-frequency atmospheric circulation patterns. *Monthly Weather Review* 115 (6), 1083–1126.
- Birks, H.J.B., 2003. Quantitative palaeoenvironmental reconstructions from Holocene biological data. In: Mackay, A., Battarbee, R., Birks, H.J.B., Oldfield, F. (Eds.), *Global Change in the Holocene*. Arnold, pp. 107–123.
- Bjune, A., Birks, H.J.B., Seppä, H., 2004. Holocene vegetation and climate history on a continental–oceanic transect in northern Fennoscandia based on pollen and plant macrofossils. *Boreas* 33, 211–233.
- Bjune, A., Bakke, J., Nesje, A., Birks, H.J.B., 2005. Holocene mean July temperature and winter precipitation in western Norway inferred from palynological and glaciological lake-sediment proxies. *The Holocene* 15 (2), 177–189.
- Bond, G., Kromer, B., Beer, J., Muscheler, R., Evans, M.N., Showers, W., Hoffmann, S., Lotti-Bond, R., Hajdas, I., Bonani, G., 2001. Persistent solar influence on North Atlantic climate during the Holocene. *Science* 294, 2130–2136.
- Calvo, E., Grimalt, J., Jansen, E., 2002. High resolution U-37(K) sea surface temperature reconstruction in the Norwegian Sea during the Holocene. *Quaternary Science Reviews* 21 (12–13), 1385–1394.
- Cassou, C., Terray, L., Hurrell, J.W., Deser, C., 2004. North Atlantic winter climate regimes: spatial asymmetry, stationarity with time, and oceanic forcing. *Journal of Climate* 17 (5), 1055–1068.
- Casty, C., Handorf, D., Raible, C.C., Gonzalez-Rouco, J.F., Weisheimer, A., Xoplaki, E., Luterbacher, J., Dethloff, K., Wanner, H., 2005. Recurrent climate winter regimes in reconstructed and modelled 500 hPa geopotential height fields over the North Atlantic/European sector 1659–1990. *Climate Dynamics* 24 (7–8), 809–822.
- Cubasch, U., Meehl, G.A., Boer, G.J., Stouffer, R.J., Dix, M., Noda, A., Seiner, C.A., Raper, S., Yap, K.S., 2001. Projections of future climate change. In: Houghton, J.T., et al. (Ed.), *Climate change 2001: the scientific basis. Contribution of working group I to the third assessment report of the intergovernmental panel on climate change*. Cambridge University Press, Cambridge, pp. 525–582.
- Dahl, S.O., Nesje, A., 1996. A new approach to calculating Holocene winter precipitation by combining glacier equilibrium-line altitudes and pine-tree limits: a case study from Hardangerjokulen, central southern Norway. *Holocene* 6 (4), 381–398.
- Dahl, S.O., Nesje, A., Lie, Ø., Fjordheim, K., Matthews, J.A., 2002. Timing, equilibrium-line altitudes and climatic implications of two early-Holocene glacier readvances during the Erdalen Event at Jostedalbreen, western Norway. *Holocene* 12 (1), 17–25.
- Dahl, S.O., Bakke, J., Lie, O., Nesje, A., 2003. Reconstruction of former glacier equilibrium-line altitudes based on proglacial sites: an evaluation of approaches and selection of sites. *Quaternary Science Reviews* 22 (2–4), 275–287.
- Dawson, A.G., Hickey, K., Holt, T., Elliott, L., Dawson, S., Foster, I.D.L., Wadhams, P., Jonsdottir, I., Wilkinson, J., McKenna, J., Davis, N.R., Smith, D.E., 2002. Complex North Atlantic Oscillation (NAO) Index signal of historic North Atlantic storm-track changes. *The Holocene* 12, 363–369.
- Dickson, R.R., Osborn, T.J., Hurrell, J.W., Meincke, J., Blindheim, J., Adlandsvik, B., Vinje, T., Alekseev, G., Maslowski, W., 2000. The Arctic Ocean response to the North Atlantic Oscillation. *Journal of Climate* 13 (15), 2671–2696.
- Graf, H.F., Walter, K., 2005. Polar vortex controls coupling of North Atlantic Ocean and atmosphere. *Geophysical Research Letters* 32. doi:10.1029/2004GL020664.
- Heegaard, E., Birks, H.J.B., Telford, R.J., 2005. Relationships between calibrated ages and depth in stratigraphical sequences: an estimation procedure by mixed-effect regression. *Holocene* 15 (4), 612–618.
- Holzhauser, H., Magny, M., Zumbuhl, H.J., 2005. Glacier and lake-level variations in west-central Europe over the last 3500 years. *Holocene* 15 (6), 789–801.
- Hurrell, J.W., 1995. Decadal trends in the North Atlantic Oscillation: regional temperatures and precipitation. *Science* 269, 676–679.
- Hurrell, J.W., Kushnir, Y., Ottersen, G., Visbeck, M., 2003. *The North Atlantic Oscillation: Climatic Significance and Environmental Impact*. Geophysical Monograph Series, vol. 134. American Geophysical Union, Washington. 279 pp.
- Hutterli, M.A., Raible, C.C., Stocker, T.F., 2005. Reconstructing climate variability from Greenland ice sheet accumulation: an ERA40 study. *Geophysical Research Letters* 32 (23).
- Jacobit, J., Wanner, H., Luterbacher, J., Beck, C., Philipp, A., Sturm, K., 2003. Atmospheric circulation variability in the North-

- Atlantic–European area since the mid-seventeenth century. *Climate Dynamics* 20 (4), 341–352.
- Jansen, E., deMenocal, P., Grousset, F. (Eds.), 2004. *Holocene Climate Variability— A Marine Perspective*. Special Issue of *Quaternary Science Review*, 23/20. Elsevier Ltd, Oxford. 2061–2268 pp.
- Karlén, W., Kuylentierna, J., 1996. On solar forcing of Holocene climate: evidence from Scandinavia. *The Holocene* 6, 359–365.
- Kim, J.H., Rambu, N., Lorenz, S.J., Lohmann, G., Nam, S.I., Schouten, S., Ruhlemann, C., Schneider, R.R., 2004. North Pacific and North Atlantic sea-surface temperature variability during the Holocene. *Quaternary Science Reviews* 23 (20–22), 2141–2154.
- Korhola, A., Vasko, K., Taivonen, H.T.T., Olander, H., 2002. Holocene temperature changes in northern Fennoscandia reconstructed from chironomids using Bayesian modelling. *Quaternary Science Reviews* 21, 1841–1860.
- Lie, O., Dahl, S.O., Nesje, A., 2003a. A theoretical approach to glacier equilibrium-line altitudes using meteorological data and glacier mass-balance records from southern Norway. *The Holocene* 13 (3), 365–372.
- Lie, O., Dahl, S.O., Nesje, A., 2003b. Theoretical equilibrium-line altitudes and glacier buildup sensitivity in southern Norway based on meteorological data in a geographical information system. *Holocene* 13 (3), 373–380.
- Luterbacher, J., Schmutz, C., Gyalistras, D., Xoplaki, E., Wanner, H., 1999. Reconstruction of monthly NAO and EU indices back to AD 1675. *Geophysical Research Letters* 26 (17), 2745–2748.
- Luterbacher, J., Xoplaki, E., Dietrich, D., Jones, P.D., T.D., D., Portis, J.F., Conzalez-Roucho, H., von Storch, H., Gyalistras, C., Casy, C., Wanner, H., 2002. Extending North Atlantic Oscillation reconstructions back to 1500. *Atmospheric Science Letters* 2 (114–124). doi:10.1006/asle.2001.0044.
- Mayewski, P.A., Rohling, E.E., Stager, J.C., Karlen, W., Maasch, K.A., Meeker, L.D., Meyerson, E.A., Gasse, F., van Kreveland, S., Holmgren, K., Lee-Thorp, J., Rosqvist, G., Rack, F., Staubwasser, M., Schneider, R.R., Steig, E.J., 2004. Holocene climate variability. *Quaternary Research* 62 (3), 243–255.
- Nesje, A., 2005. Briksdalsbreen in western Norway: AD 1900–2004 frontal fluctuations as a combined effect of variations in winter precipitation and summer temperature. *Holocene* 15 (8), 1245–1252.
- Nesje, A., Kvamme, M., Rye, N., Løvlie, R., 1991. Holocene glacial and climate history of the Jostedalbreen region, western Norway; evidence from lake sediments and terrestrial deposits. *Quaternary Science Reviews* 10, 87–114.
- Nesje, A., Dahl, S.O., Andersson, C., Matthews, J.A., 2000a. The lacustrine sedimentary sequence in Syngneskardvatnet, western Norway: a continuous, high-resolution record of the Jostedalbreen ice cap during the Holocene. *Quaternary Science Reviews* 19 (11), 1047–1065.
- Nesje, A., Lie, O., Dahl, S.O., 2000b. Is the North Atlantic Oscillation reflected in Scandinavian glacier mass balance records? *Journal of Quaternary Science* 15 (6), 587–601.
- Nesje, A., Matthews, J.A., Dahl, S.O., Berrisford, M.S., Andersson, C., 2001. Holocene glacier fluctuations of Flatebreen and winter-precipitation changes in the Jostedalbreen region, western Norway: evidence from pro-glacial lacustrine sediment records. *Holocene* 11 (3), 267–280.
- Nesje, A., Jansen, E., Birks, H.J.B., Bjune, A., Bakke, J., Dahl, C.A., Dahl, S.O., Kiltgaard-Kristensen, D., Lauritzen, S.E., Lie, Ø., Risebrobakken, B., Svendsen, J.I., 2005. Holocene climate variability in the northern North Atlantic region: a review of terrestrial and marine evidence. In: Drange, H., Dokken, T., Furevik, T., Rüdiger, G., Bergen, W. (Eds.), *The Nordic Seas: An integrated Perspective*. Geophysical Monograph Series, pp. 289–322.
- Nesje, A., Bakke, J., Dahl, S.O., Lie, O., Matthews, J.A., 2007-this issue. Norwegian mountain glaciers in the past, present and future. *Global and planetary change*. doi:10.1016/j.gloplacha.2006.08.004
- Nordli, O., Lie, O., Nesje, A., Benestad, R.E., 2005. Glacier mass balance in southern Norway modelled by circulation indices and spring–summer temperatures AD 1781–2000. *Geografiska Annaler. Series A. Physical Geography* 87A (3), 431–445.
- O'Brien, S.R., Mayewski, P.A., Meeker, L.D., Meese, D.A., Twickler, M.S., Whitlow, S.I., 1995. Complexity of Holocene climate as reconstructed from a Greenland ice core. *Science* 270 (5244), 1962–1964.
- Oerlemans, J., 2005. Extracting a climate signal from 169 glacier records. *Science* 308 (5722), 675–677.
- Ostermeier, G.M., Wallace, J.M., 2003. Trends in the North Atlantic Oscillation–Northern Hemisphere annular mode during the twentieth century. *Journal of Climate* 16 (2), 336–341.
- Renssen, H., Goosse, H., Fichet, T., Brovkin, V., Driesschaert, E., Wolk, F., 2005. Simulating the Holocene climate evolution at northern high latitudes using a coupled atmosphere–sea ice–ocean–vegetation model. *Climate Dynamics* 24 (1), 23–43.
- Risebrobakken, B., Jansen, E., Andersson, C., Mjelde, E., Hevrøy, K., 2003. A high-resolution study of Holocene paleoclimatic and paleoceanographic changes in the Nordic Seas. *Paleoceanography* 18, 1017–1029.
- Rogers, J.C., 1997. North Atlantic storm track variability and its association to the North Atlantic Oscillation and climate variability of Northern Europe. *Journal of Climate* 10, 1635–1647.
- Rosqvist, G., Jonsson, C., Yam, R., Karlen, W., Shemesh, A., 2004. Diatom oxygen isotopes in pro-glacial lake sediments from northern Sweden: a 5000 year record of atmospheric circulation. *Quaternary Science Reviews* 23 (7–8), 851–859.
- Seppä, H., Birks, H.J.B., 2001. July mean temperature and annual precipitation trends during the Holocene in the Fennoscandian tree-line area: pollen-based climate reconstructions. *The Holocene* 11, 527–539.
- Seppä, H., Birks, H.J.B., 2002. Holocene climate reconstructions from the Fennoscandian Tree-Line Area based on pollen data from Toskaljävri. *Quaternary Research* 57, 191–199.
- Seppä, H., Birks, J.H.H., Odland, A., Poska, A., Veski, S., 2004. A modern pollen-climate calibration set from northern Europe: developing and testing a tool for palaeoclimatological reconstructions. *Journal of Biogeography* 31, 251–267.
- Shabbar, A., Huang, J.P., Higuchi, K., 2001. The relationship between the wintertime North Atlantic Oscillation and blocking episodes in the North Atlantic. *International Journal of Climatology* 21 (3), 355–369.
- Sissons, J.B., 1979. The Loch Lomond stadial in the British Isles. *Nature* 280, 199–203.
- Sutherland, D.G., 1984. Modern glacier characteristics as a basis for inferring former climates with particular reference to the Loch Lomond stadial. *Quaternary Science Reviews* 3, 291–309.
- Timmermann, A., Goosse, H., 2004. Is the wind stress forcing essential for the meridional overturning circulation? *Geophysical Research Letters* 31. doi:10.1029/2003GL018777.
- Walter, K., Graf, H.F., 2005. The North Atlantic variability structure, storm tracks, and precipitation depending on the polar vortex strength. *Atmospheric Chemistry and Physics* 5, 239–248.